Synthesis and Characterization of Germanium/Si−Alkyl and Germanium/Silica Core−Shell Quantum Dots

Chung-Sung Yang and Susan M. Kauzlarich*

Department of Chemistry, University of California, One Shields Avenue, Davis, California 95616

Y. C. Wang†

National Center for Electron Microscopy, Lawrence Berkeley National Laboratory, Berkeley, California 94720

Received September 17, 1999

Ge/Si−R and Ge/SiO_2 core−shell nanoparticles have been synthesized by a solution route from the stepwise reactions of the Zintl salt, Mg_2Ge, with $SiCl_4$ and subsequently either RLi (R = butyl) or H_2O_2. High-resolution transmission electron microscopy (HRTEM) images show that the core part of these Ge/Si−R and Ge/SiO_2 nanoparticles is crystalline and the *d* spacing of lattice fringes agrees with the {111} crystal plane (3.27 Å) of Ge. The average sizes (diameter) are 5.8(2.3) and 6.8(2.8) nm for Ge/Si−R and Ge/SiO_2, respectively. Fourier transform−infrared (FTIR) spectra are consistent with alkyl groups bonded to the silicon surface in Ge/Si−R nanoclusters. Off-axis holography was performed for several Ge/SiO_2 nanoparticles. The characterization of the ratio of radii and geometry between the core part and the outer sphere of Ge/SiO_2 is presented. The reconstructed phase image from the hologram offers detailed information concerning the ratio of the shell thickness ($R - r$) to the radius of the core (r), Rr = $(R - r)/r$, by measuring the phase shift and the resultant phase contrast. The Rr value from the deconvoluted phase image of a 16 nm spherelike Ge/SiO_2 is 0.264 (0.065). Photoluminescence (PL) spectra of both Ge/Si−R and Ge/SiO_2 nanoclusters show a strong UV−blue PL with a peak centered between 400 and 410 nm. These results suggest that the UV−blue PL may be attributed to the core part of these nanoparticles.

Introduction

Semiconductor nanoclusters have received much attention in recent years, because of their potential applications in the fabrication of optoelectronic devices.[1,2] Solid-state lasers, flat panel displays, light emitting diodes, and optoelectronic sensors using nanoscaled electronic circuitry are some examples of current applications of semiconductor nanocluster research. The bulk of research on semiconductor nanoclusters focuses on the II−VI and III−V binary semiconductors due to the direct-gap band structure.[3−6] Recently, silicon and germanium nanoclusters have attracted a great deal of interest because of the surprising discovery that nanoparticles of silicon and germanium can be made to luminescence in the visible region.[7−21] There has also been significant interest in understanding how quantum confinement effects will be manifested in indirect-gap semiconductors.[22−27] Unlike the intense research on

† Current address: FEI Company, Applications Laboratory, 7451 N. W. Evergreen Parkway, Hillsboro, OR 97124.

(1) For example, see: *MRS* **1998**, *23*, 16.
(2) Brus, L. E. *Semiconductor Nanocrystals, Microelectronics, and Solar Cells*; Laudise, R. A., Ed.; Houston, Texas, 1995; p 21.
(3) Henglein, A. *Chem. Rev.* **1989**, *89*, 1861.
(4) Steigerwald, M. L.; Brus, L. B. *Annu. Rev. Mater. Sci.* **1989**, *19*, 471.
(5) Wang, Y.; Herron, N. *J. Phys. Chem.* **1991**, *95*, 525.
(6) Steigerwald, M. L.; Brus, L. E. *Acc. Chem. Res.* **1990**, *23*, 183.
(7) Cullis, A. G.; Canham, L. T.; Calcott, P. D. J. *J. Appl. Phys.* **1997**, *82*, 909.
(8) Fojtik, A.; Weller, H.; Fiechter, S.; Henglein, A. *Chem. Phys. Lett.* **1987**, *134*, 477.
(9) Ito, T.; Ohta, T.; Hiraki, A. *Jpn. J. Appl. Phys.* **1992**, *31*, L1.
(10) Littau, K. A.; Szajowshki, P. J.; Muller, A. J.; Kortan, A. R.; Brus, L. E. *J. Phys. Chem.* **1993**, *97*, 1224.
(11) Wilson, W. L.; Szajowski, P. F.; Brus, L. E. *Science* **1993**, *262*, 1242.
(12) Koch, F.; Petrova-Koch, V.; Muschik, T. *J. Lumin.* **1993**, *57*, 271.
(13) Morisaki, H.; Hashimoto, H.; Ping, F. W.; Nozawa, H.; Ono, H. *J. Appl. Phys.* **1993**, *74*, 2977.
(14) Fojtik, A.; Henglein, A. *Chem. Phys. Lett.* **1994**, *221*, 363.
(15) Brus, L. E.; Szajowski, P. F.; Wilson, W. L.; Harris, T. D.; Schuppler, S.; Citrin, P. H. *J. Am. Chem. Soc.* **1995**, *117*, 2915.
(16) Maeda, Y.; Tsukamoto, N.; Yazawa, Y.; Kanemitsu, Y.; Masumoto, Y. *Appl. Phys. Lett.* **1991**, *59*, 3168.
(17) Maeda, Y. *Phys. Rev. B* **1995**, *51*, 1658.
(18) Dutta, A. K. *Appl. Phys. Lett.* **1996**, *68*, 1189.
(19) Bley, R. A.; Kauzlarich, S. M.; Davis, J. E.; Lee, H. W. H. *Chem. Mater.* **1996**, *8*, 1881.
(20) Taylor, B. R.; Kauzlarich, S. M.; Lee, H. W. H.; Delgado, G. R. *Chem. Mater.* **1998**, *10*, 22.
(21) Dhas, N. A.; Raj, C. P.; Gedanken, A. *Chem. Mater.* **1998**, *10*, 3278.
(22) Proot, J. P.; Delerue, C.; Allan, G. *Appl. Phys. Lett.* **1992**, *61*, 1948.
(23) Zhang, D.; Kolbas, R. M.; Mehta, P.; Singh, A. K.; Lichtenwalner, D. J.; Hsieh, K. Y.; Kingon, A. I. *Mater. Res. Soc. Symp. Proc.*, MRS, **1992**, *256*, 35.
(24) Zhang, S. B.; Zunger, A. *Appl. Phys. Lett.* **1993**, *63*, 1399.
(25) Delerue, C.; Allan, G.; Martin, E.; Lannoo, M. *Theory of Silicon Crystallites, in Porous Silicon Science and Technology*; Springer-Verlag: New York, 1995.
(26) Hybertsen, M. S. *Phys. Rev. Lett.* **1994**, *72*, 1514.
(27) Iyer, S. S.; Xie, Y.-H. *Science* **1993**, *260*, 40.

10.1021/cm9905949 CCC: $18.00
Published on Web 11/06/1999

nano-Si, there has been much less on Ge nanoparticles. This is rather surprising considering that bulk Ge has a larger dielectric constant and smaller carrier masses compared to bulk Si. In addition, Ge barely misses being a direct gap semiconductor. Because of these facts, one might expect that the quantum confinement effect would appear more pronounced in Ge than that in Si.

Synthetic approaches to Si and Ge nanoparticles have recently been reviewed.[28] There are only a few solution routes, and none of them, so far, have yielded the size control that can be demonstrated with the II−VI nanoclusters. However, solution methods have the potential for high yields, size control, and control of surface.[20,29−32] In this paper, a study of the newly synthesized Ge/Si−R and Ge/SiO_2 core−shell nanoclusters is reported. The Ge/Si core/shell provides an effective capping of the Ge surface, similar to CdSe/ZnS core/shell nanoparticles.[33] The further termination with alkyls protects the Si surface from oxidation and allows these Ge nanoparticles to be soluble in a variety of organic solvents, thus making them amenable for polymer blends in device applications. The SiO_2 termination provides a different surface modification that allows us to probe the photoluminescence (PL) of these nanoparticles with different surfaces. The SiO_2 termination also provides an alternate surface that can be further modified to make more complex arrays of nanoparticles attached to surfaces or polymers. The synthesis of these two types of core−shell nanoparticles illustrates that complex core−shell structures are obtainable by solution synthetic methods with group IV semiconductors similar to what has been reported for silica-coated metal nanoparticles.[34] These core−shell nanoparticles are new materials with potential use in structural and functional applications for the next generation nanophase or cluster-assembled nanostructured materials.

Experimental Section

The nanoclusters were synthesized via a solution synthesis route developed by this group.[20,32,35−38] The reaction of $SiCl_4$ with Mg_2Ge is performed under a Schlenk line Ar atmosphere in tri(ethylene glycol) dimethyl ether (triglyme). This reaction produces nanometer-sized Ge/Si−Cl crystallites with a chloride-passivated surface. The reaction was allowed to reflux for 6 h. Further reaction with alkyllithium (RLi) provides a stable surface terminated with alkyls (Ge/Si−R). The resultant crystalline particles can be suspended in organic solvent, such as hexane or cyclohexane, or isolated as a powder. The Ge/SiO_2 nanoclusters are synthesized in ethylene glycol dimethyl ether (glyme). The synthesis route is similar to that of Ge/Si−R nanoparticles. After the reaction of $SiCl_4$ with Mg_2Ge in glyme for 72 h, 30% H_2O_2 is added and the solution is allowed to reflux for one more hour. The pale-yellow crystalline particles can be precipitated and dried as a powder or suspended in ethanol. X-ray powder diffraction data were obtained on an Inel 3000. Data were collected at room temperature using Cu $K\alpha_1$ radiation with a position-sensitive detector. High-resolution transmission electron microscope images and electron holograms were collected using a 300 keV Philips CM300 UT/FEG TEM equipped with a Schottky field-emission source. Samples were prepared by evaporation of colloids onto lacy carbon-coated 200 mesh grids. Fourier transform−infrared (FTIR) spectra were obtained at room temperature by dropping the hexane colloid onto a CsI plate and allowing the solvent to evaporate. The spectra were collected on a Mattson Galaxy series FTIR 3000 spectrophotometer. Photoluminescence spectra were obtained with a Perkin-Elmer LS 50B luminescence spectrophotometer.

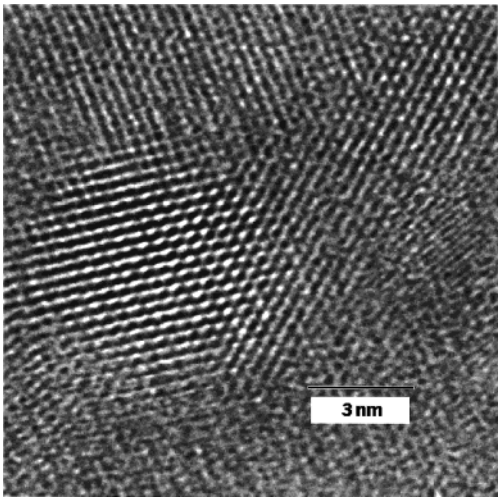

Figure 1. HRTEM image showing the Ge/Si-*n*-butyl core/shell nanoclusters. *D* spacing of the lattice fringes for the central part measures 3.27 Å, consistent with germanium {111} crystal planes.

Results and Discussion

The HRTEM image in Figure 1 of Ge/Si−*n*-butyl shows that the core part of the nanoclusters is crystalline and is consistent with Ge lattice fringes of the {111} crystal plane (3.27 Å). However, the outer sphere layer (Si) could not be confirmed on the basis of HRTEM. Characterization of the Ge/Si interface in these nanoparticles would require specialized techniques such as spatially resolved EELS (electron energy loss spectroscopy),[39] or QuantiTEM (quantitative TEM) methods,[40] because the *d* spacing lattice mismatch for {111} crystal plane between Si (3.1340 Å) and Ge (3.2667 Å) is only 0.1327 Å (4.23%). The resolution limit of conventional HRTEM cannot resolve such a subtle lattice mismatch at the interface of these small nanoparticles. Therefore, evidence for a Si−R surface on Ge is inferred based on HRTEM showing that the core part is Ge, FTIR spectroscopy showing alkyl stretches, and the subsequent synthesis of Ge/SiO_2 nanoparticles. FTIR spectroscopy is used to verify the surface termination while photo-

(28) King, W. D.; Boxall, D. L.; Lukehart, C. M. *J. Cluster Sci.* **1997**, *8*, 267.
(29) Kornowski, A.; Giersig, M.; Vogel, R.; Chemseddine, A.; Weller, H. *Adv. Mater.* **1993**, 634.
(30) Heath, J. R.; LeGoues, F. K. *Chem. Phys. Lett.* **1993**, *208*, 263.
(31) Heath, J. R.; Shiang, J. J.; Alivisatos, A. P. *J. Chem. Phys.* **1994**, *101*, 1607.
(32) Taylor, B. R.; Kauzlarich, S. M.; Delgado, G. R.; Lee, H. W. H. *Chem. Mater.* **1999**, *11*, 2493.
(33) Kortan, A. R.; Hull, R.; Opila, R. L.; Bawendi, M. G.; Steigerwald, M. L.; Carroll, P. J.; Brus, L. E. *J. Am. Chem. Soc.* **1990**, *112*, 1327.
(34) Liz-Marzán, L. M.; Giersig, M.; Mulvaney, P. *Langmuir* **1996**, *12*, 4329.
(35) Bley, R. A.; Kauzlarich, S. M. *J. Am. Chem. Soc.* **1996**, *118*, 12461.
(36) Bley, R. A.; Kauzlarich, S. M. *A New Solution Phase Synthesis for Silicon Nanoclusters*; Fendler, J. H., Dékány, I., Eds.; Kluwer Academic Press: Dordrecht, The Netherlands, 1996; p 467.
(37) Bley, R. A.; Kauzlarich, S. M. *Synthesis of Silicon Nanoclusters*; Fendler, J. H., Ed.; Wiley-VCH: Weinheim, 1998; p 101.
(38) Yang, C.-S.; Kauzlarich, S. M.; Lee, H. W. H.; Delgado, G. R. *J. Am. Chem. Soc.* **1999**, *121*, 5191.
(39) Batson, P. E.; Heath, J. R. *Phys. Rev. Lett.* **1993**, *71*, 911.
(40) Schwander, P.; Rau, W.-D.; Ourmazd, A. *J. Microsc.* **1998**, *190*, 171.

Table 1. Characteristic Infrared Stretches Observed in Ge/Si-*n*-Butyl Nanoclusters

wavenumbers cm $^{-1}$ (intensity)[a]	functional group[b]
2970−2960 (m)	C−CH_3 terminal, ···CH_3 asymmetric stretching
2920−2890 (s)	CH_2 stretching
2860−2840 (s)	C−CH_3 terminal, ···CH_3 symmetrical stretching
1460−1450 (m)	Si···CH_2 scissor, or C−CH_3 deformation
1360−1340 (w)	C···H deformation or bending

[a] s = strong, m = medium, and w = weak. [b] From Lin et al. [46] and Socrates[47]

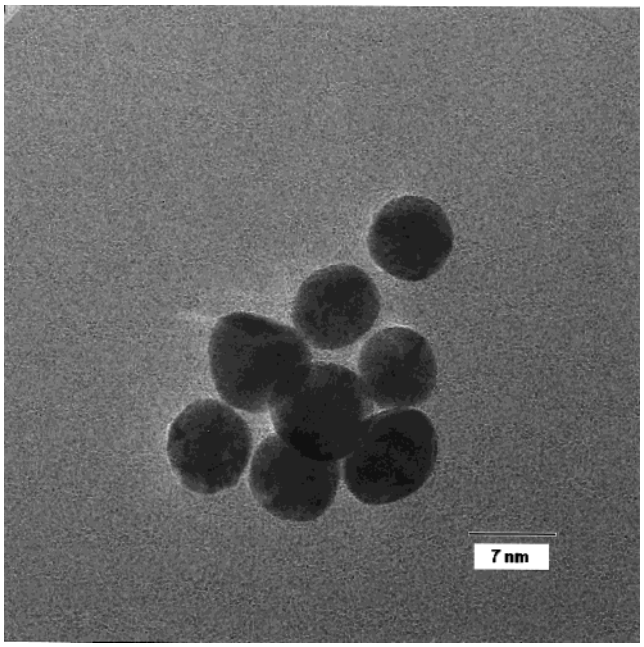

Figure 2. Micrograph with some typical sizes of Ge/SiO_2 core/shell nanoparticles.

luminescence spectroscopy is employed to investigate the optical properties of the core. Five characteristic IR peaks were observed in Ge/Si-*n*-butyl spectrum: 2970−2960, 2920−2890, 2860−2840, 1460−1450, and 1360−1340 cm^{-1}. These peaks are assigned to the functional groups shown in Table 1. The results obtained from the FTIR spectrum suggest that the surface of Si capped Ge nanoclusters is alkyl-terminated and oxygen-free.

Figure 2 shows a micrograph for Ge/SiO_2 that contains some typical sizes of nanoparticles. Similar shapes and variety of sizes were observed in other preparations. The histogram of size distribution of Ge/Si-*n*-butyl and Ge/SiO_2 derived from nine TEM images is shown in Figure 3. The average size of nanoparticles (diameter) is 5.8 nm with a standard deviation of 2.3 nm for Ge/Si−R and an average diameter of 6.8(2.8) nm for Ge/SiO_2. This reaction does not employ the use of micelles to control size, and therefore the size distributions show rather large standard deviations. Figure 4 shows a typical X-ray powder diffraction pattern obtained from the Ge/SiO_2 preparation. The (111) and (220) reflections of Ge are clearly observed. The full width at half-maximum of the peaks is narrow, reflecting the diffraction of the larger particles in the sample.

A HRTEM image for an approximately 31 nm diam, oval-like Ge/SiO_2 nanoparticle is shown in Figure 5.

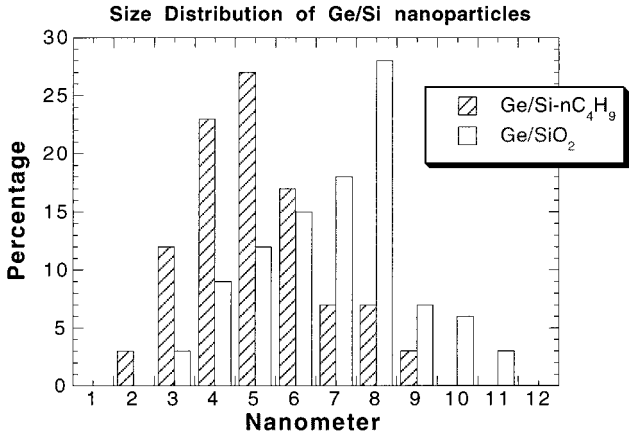

Figure 3. Size distribution of Ge/Si-*n*C_4H_9 and Ge/SiO_2 from nine TEM images. The average sizes (diameter) of nanoparticles are 5.8(2.3) and 6.8(2.8) nm for Ge/Si-*n*C_4H_9 and Ge/SiO_2, respectively.

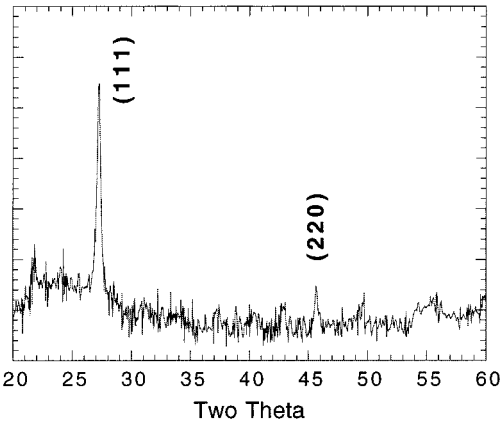

Figure 4. X-ray powder diffraction pattern of the Ge/SiO_2 core/shell nanoparticles.

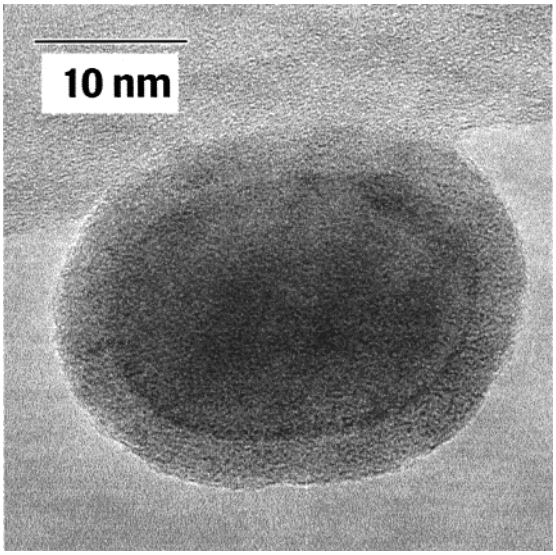

Figure 5. HRTEM image for a 31 nm diam, oval-like, SiO_2 capped Ge nanoparticle. Both the outer shell and core part are clearly shown.

Nanoparticles of this size are rare, with most observed in the TEM being between 1 and 10 nm; see Figure 3. This type of image offers the best opportunity to study the geometry of a core−shell nanoparticle. Images such as this for the Ge/SiO_2 particles are possible due to the

Table 2. Mean Inner Potential (MIP)[a] for Si and Ge and Their Oxides[b]

specimen	calculated MIP	experimental data
Si	13.943	12.1 ± 1.3[c]
Ge	15.668	
Ge−O_2	19.504	
Si −O_2 (amorphous)	10.334	10.0 ± 0.6[c]
Si −O_2 (quartz)	12.451	

[a] Where MIP = $(47.878/\Omega) \times \Sigma F^B$. ($F^B$ = structure factor calculated from electron scattering factors. If scattering angle = 0, Si = 5.828, Ge = 7.378, C= 2.509, H = 0.529, O = 1.983.) [b] Ω = scattering volume (= unit cell in the case of a crystalline material). Crystalline Si: $\Omega = (5.429)^3/8 = 20.013$. Crystalline Ge $\Omega = (5.565)^3/8 = 22.545$. [c] From Wang et al. [43]

static interaction between the SiO_2 surface and the lacy carbon grid. It is very difficult for us to obtain similar images for the Ge/Si−R nanoparticles. This might be expected, because the alkyl surfaces are expected to have little or no affinity for the carbon substrate. The region with uniform gray contrast corresponds to the normalized background of the vacuum. Both outer sphere and core are clearly shown, but the precise center of the image is unknown. The *d* spacing of lattice fringes of the core part (3.27 Å) match the Ge {111} crystal plane, and selected area electron diffraction (SAED) confirms the polycrystalline structure of Ge. The lattice fringes of the outer shell are not discernible, and no crystalline diffraction was seen in the SAED of this part. These results suggest that the core/shell geometry of Ge/SiO_2 nanoparticle contains a polycrystalline core part (Ge) and an amorphous outer sphere (SiO_2).

The image information from a conventional HRTEM is based on the recorded intensity of an electron beam, the amplitude component. The use of off-axis electron holography is an alternative way to verify the structure because a hologram contains both amplitude and phase information.[41,42] The reconstructed phase image from the hologram is able to offer detailed information for the radii of the Ge and SiO_2 sphere by measuring the phase shift and the resultant phase contrast.[43] The ratio of radii, Rr, value is the ratio of the thickness of the shell to the radius of the core and is defined as $Rr = (R - r)/r$, where R is the radius of the particle and r is the radius of the core. The Rr value can be obtained from the deconvoluted phase image.

The relationship between specimen radius, or thickness, phase shift of the electron wave passing through the sample, and mean inner potential in the absence of dynamical diffraction effects is shown in the following equation:

$$\Delta\phi = (1/C_E)\Phi_0 t \quad (1)$$

where $\Delta\phi$ is the phase shift of the electron wave and t is the specimen thickness (nm) in the beam direction. C_E is an energy-dependent constant (=153.1712 nm V/rad for 300 keV accelerating voltage). Φ_0 is the mean inner potential (MIP). The MIP of a solid effectively represents the volume average of the atomic potential depending on composition, bonding, and structure. Methods for Φ_0 measurement have relative errors reported to be in the range of 2.5% to about 10%. The calculated surface density and MIP data are listed in Table 2. The potential difference of 5.334 V for Ge/SiO_2 will result in an obvious phase contrast for Rr calculation.

A reconstructed phase image from the hologram of an approximately 16 nm diam, spherelike Ge/SiO_2 nanoparticle is shown in Figure 6a. Although this nanoparticle is very close to spherical, the precise center

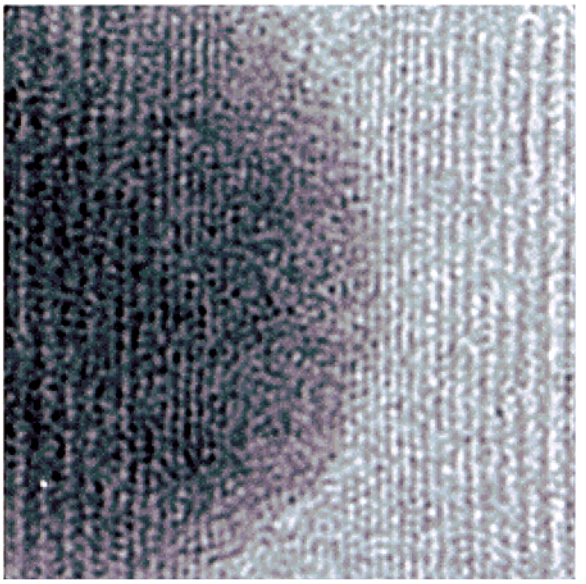

(a)

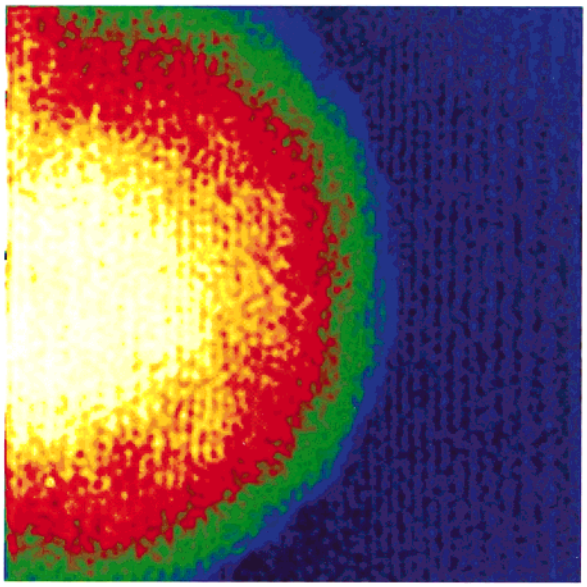

(b)

Figure 6. (a) Phase image reconstructed from the hologram of a 16 nm spherical Ge/SiO_2 nanoparticle. (b) Deconvoluted color phase image of part a. Different colors represent different MIP areas. The yellow-orange area represents Ge, and the green-blue area is for the SiO_2 layer. The average phase shift in a vacuum (dark part) is set to zero. The Rr value derived from this phase image is 0.264(0.065).

(41) Tonomura, A. *Electron Holography*; Springer-Verlag: Berlin, 1993; Vol. 70.
(42) Tonomura, A.; Allard, L. F.; Pozzi, G.; Joy, D. C.; Ono, Y. A. *Electron Homography*; Elsevier Science B. V.: Amsterdam, 1995.
(43) Wang, Y. C.; Chou, T. M.; Libera, M.; Kelly, T. F. *Appl. Phys. Lett.* **1997**, *70*, 1296.

of the particle is unknown. Being unable to remove Fresnel fringes completely due to the drifting of the electron biprism, faint periodic modulations are visible in the reconstructed phase image. The average phase shift in a vacuum (dark part) is set to zero for normalization. The error of measurement for the diameter can be introduced in experimental images when the sphere edge is difficult to define precisely. Deviations from a crystalline nanosphere due to faceting and dynamical scattering may also increase relative error.[44] It is experimentally difficult to tilt such a small specimen to a weakly scattering orientation. In this particular case, error induced by the SiO_2 surface layer is relatively small because its thickness is much less than the Ge core.[43] The line plot of the phase diagram of this reconstructed image shows that the SiO_2 capping of Ge is complete because the phase shift between Ge and SiO_2 interphase is dramatic, with an obvious change of slope. Figure 6b shows a deconvoluted color phase image of Figure 6a. Different coded colors represents different MIP areas. The yellow-orange area represents the core part Ge, and the green-blue area is the outer sphere SiO_2 layer. The Rr value for SiO_2 to Ge derived from this phase image is 0.264 with a standard derivation of 0.065. It is also found in several other samples that the smaller the nanoparticles the larger the Rr values.

The synthesis of Ge nanoparticles with two different surfaces allows us to study the effect of surface on the photoluminescence. Ge/R nanoparticles show blue PL that is attributed to quantum confinement.[20,32,45] In the PL spectra, a strong UV−blue PL ranging from 360 to 550 nm is observed for both Ge/Si-*n*-butyl and Ge/SiO_2 nanoparticles, as shown in Figure 7. The center of the UV−blue peak is located at 400−410 nm, or 3.0−3.1 eV, with an excitation wavelength of 310 nm and shows a continuous shift with the increase of excitation wavelength. This is a different spectral region from other blue emitters, such as oxidized silicon (440−480 nm) or silicon carbide (500−520 nm). This is similar to the data reported on alkyl-terminated Ge nanoclusters[20,32,45] and provides convincing evidence that the PL is intrinsic to the core part of the nanoparticle.

In summary, the Ge/Si nanoparticles terminated with *n*-butyl groups or further oxidized to silica have been investigated in order to understand the role of surface in the UV−blue PL. The HRTEM images show that the core part of these nanoparticles is crystalline and is consistent with germanium lattice fringes of the crystal plane {111} (3.27 Å). X-ray powder diffraction provides additional support for a crystalline Ge core. A HRTEM micrograph of a 31 nm diam Ge/SiO_2 nanoparticle shows a clear image for both outer sphere and core part. The reconstructed phase image from the hologram shows that the germanium is completely capped with SiO_2. The Rr value of a 16 nm spherelike Ge/SiO_2 nanoparticle derived from a deconvoluted color phase image is 0.264 (0.065). PL spectra of the nanoclusters show a strong UV−blue PL with a maximum between 400 and 410 nm. UV−blue PL can be observed in nanoparticles regardless of the surface termination suggesting that the PL is intrinsic to the Ge core.

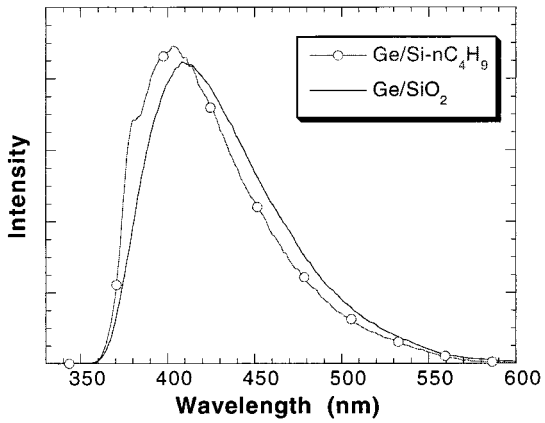

Figure 7. PL spectra for Ge/Si−*n*-butyl and Ge/SiO_2 core/shell nanoparticles. These emission spectra were collected from 300 to 800 nm with an excitation bandwidth of 2.5 nm and excitation wavelength of 310 nm. The maximum is centered between 400 and 410 nm or 3.0−3.1 eV.

Acknowledgment. The authors are grateful to the National Science Foundation (Grant No. DMR-9803074) and Campus Laboratory Collaboration Program of the University of California for financial support. Work was performed under the auspices of the U.S. Department of Energy by Lawrence Livermore National Laboratory under Contract W-7405-Eng-48. Work at the NCEM was performed under the auspices of the Director, Office of Energy Research, Office of Basic Energy Science, Materials Science Division, U.S. Department of Energy under Contract DE-AC-03-76-XF00098.

CM9905949

(44) Gajdardziska-Josifovska, M.; MaCartney, M.; de Ruijter, W. J.; Smith, D. J.; Weiss, J. K.; Zuo, J. M. *Ultramicroscopy* **1993**, *55*, 397.

(45) Delgado, G. R.; Lee, H. W. H.; Taylor, B. R.; Kauzlarich, S. M. *Phys. Rev. B*, submitted for publication.

(46) Lin, W. L.; Tsai, H. K.; Lee, S. C.; Sah, W. J.; Tzeng, W. J. *Appl. Phy. Lett.* **1987**, *51*, 2112.

(47) Socrates, G. *Infrared Characteristic Group Frequencies*; Wiley: New York, 1980.